TWO-DIMENSIONAL STUDIES OF ELECTRON BERNSTEIN WAVE EMISSION IN MAST

V. F. SHEVCHENKO,[a]* M. DE BOCK,[a] S. J. FREETHY,[a,b] A. N. SAVELIEV,[c] and R. G. L. VANN[b]

[a]*EURATOM/CCFE Fusion Association, Culham Science Centre, Abingdon, Oxon OX14 3DB, United Kingdom*
[b]*University of York, Heslington, York YO10 5DD, United Kingdom*
[c]*Ioffe Institute, Politekhnicheskaya 26, 194021 St. Petersburg, Russia*

Received July 2, 2010
Accepted for Publication August 31, 2010

Angular scanning of electron Bernstein wave emission (EBE) has been conducted in MAST. From EBE measurements over a range of viewing angles, the angular position and orientation of the B-X-O mode conversion (MC) window can be estimated, giving the pitch angle of the magnetic field in the MC layer. The radial position of the corresponding MC layer is found from Thomson scattering measurements. Measurements at several frequencies can provide a pitch angle profile. Results of pitch angle profile reconstruction from EBE measurements are presented in comparison with motional Stark effect measurements. Microwave imaging of the B-X-O MC window is proposed as an alternative to angular scanning. The proposed scheme is based on an imaging phased array of antennas allowing the required angular resolution. Image acquisition time is much shorter than magnetohydrodynamic (MHD) time scales so the EBE imaging can be used for pitch angle measurements even in the presence of MHD activity.

KEYWORDS: *spherical tokamak, q* profile, electron Bernstein wave

Note: The figures in this paper are in color only in the electronic version.

I. INTRODUCTION

MAST is a tight aspect ratio ($A = R/a = 0.85$ m/0.65 m ~ 1.3, $I_p \leq 1.5$ MA) spherical tokamak[1] (ST). The hot $T_e \leq 3$ keV, dense $n_e \leq 1 \times 10^{20}$ m^{-3}, and highly shaped ($\delta \leq 0.5$, $1.6 \leq \kappa \leq 2.5$) plasmas are accessed at moderate toroidal field $B_t(R = 0.7\ \text{m}) \leq 0.62$ T. Usually the plasma is well overdense in STs, i.e., $\omega_{pe} \gg \omega_{ce}$, where ω_{pe} and ω_{ce} are the electron plasma and electron cyclotron (EC) frequencies, respectively. In such plasmas the core is inaccessible for transverse electromagnetic waves in the range of low EC harmonics. Consequently, methods that are well established in conventional tokamaks and stellarators such as EC emission–based diagnostics and EC resonance heating and current drive cannot be employed in STs. In the past decade there has been a growing interest in utilizing electron Bernstein waves (EBWs) in overdense plasmas for these techniques.

*E-mail: vladimir.shevchenko@ccfe.ac.uk

EBWs are predominantly electrostatic waves. They cannot propagate in vacuum but they can propagate in overdense plasmas, and they are coupled to the electromagnetic extraordinary (X) and ordinary (O) modes via mode conversion (MC) mechanisms. These MC mechanisms allow the thermal EBW emission (EBE) to escape the plasma, and conversely, EBWs can be excited within the plasma with externally launched X or O modes. Hence, EBWs are considered to be a promising means for plasma diagnostics, plasma start-up, and plasma heating and current drive in STs (Refs. 2, 3, and 4). A comprehensive review of experiments with EBWs in fusion devices can be found in Ref. 5.

The present paper describes one particular diagnostic application of EBWs, namely, *q*-profile measurements in overdense plasmas. One of the possibilities of using EBWs for this purpose was proposed in Ref. 6 and experimentally verified in Refs. 7, 8, and 9. Here we develop a novel approach based on two-dimensional (2-D) measurements of the MC in ST plasmas. Some aspects of this technique were discussed by Volpe in Ref. 10. Section II of this paper presents proof-of-principle experiments supporting the

proposed technique. Section III describes the experimental setup for the pilot experiments with microwave imaging of the MC window and discusses problems related to the image reconstruction and the imaging system design. Section IV summarizes our results and conclusions.

II. ANGULAR SCANNING OF EBE IN MAST

Feasibility studies of thermal EBE measurements as a potential edge current diagnostic have been conducted on the MAST tokamak. A broadband radiometer covering the range from 7 to 40 GHz was used as a receiver. In front of the radiometer antenna a fast rotating mirror (FRM) was installed, providing a continuous scanning of the viewing direction.[10] Figure 1 illustrates the relative position of the Bernstein-extraordinary-ordinary (B-X-O) MC window in the MAST plasma and the range of viewing angles covered by the radiometer with FRM. From EBE measurements for a range of viewing angles, the optimum viewing direction for B-X-O MC can be found, giving the pitch angle of the magnetic field in the MC layer, at the position where $\omega = \omega_{pe}$. EBE measurements at several frequencies allow a pitch angle profile to be reconstructed.

Preliminary experiments with the FRM have shown that in the range of EC frequencies, thermal emission from the overdense plasma is highly anisotropic.[11,12] The resultant signal modulation due to FRM rotation is a combination of a number of factors: geometric modulation, the presence of stray radiation in the vessel, and finally anisotropic thermal EC and EBW emission. The range of viewing angles was limited in these first experiments because of the large horn antenna employed. The antenna opening of 100 mm was comparable with the FRM and vacuum window aperture in these preliminary experiments. As a result geometrical effects were responsible for a significant fraction of signal modulation.

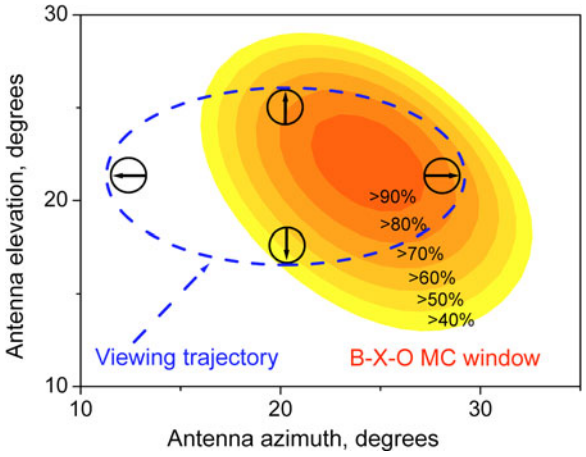

Fig. 1. Angular range covered by the FRM and the B-X-O MC window calculated for 16 GHz and pitch angle of 40 deg.

To increase the range of viewing angles, the large horn antenna has been replaced with a very compact antenna.[a] The new antenna receives two linear polarizations simultaneously in the frequency range from 6 to 40 GHz. It has an aperture of 50 mm, which is half the vacuum window size, and thus the effect of geometrical modulation has been suppressed in the whole frequency range of the radiometer.

Figure 2 illustrates radiometer signals measured during ELM-free H-mode in MAST. These signals were recorded simultaneously at vertical and horizontal polarizations at 16 GHz during one period of FRM rotation. The B-X-O MC efficiency is shown for comparison. MC was estimated using a formula derived within Wentzel-Kramers-Brillouin (WKB) approximation. This formula takes into account magnetic shear effects.[13] The density profile was obtained from high resolution Thomson scattering (TS) measurements. The shape of both signals is very close to that predicted by theory. One can see that both signals have dual maxima, indicating that the optimum viewing angles for B-X-O MC are inside the ellipse scanned by the radiometer with FRM. The amplitudes of the signals are similar near the maxima, indicating that the polarization of the registered emission is close to circular, which corresponds to the oblique O mode. Near the minima the signal with vertical polarization is stronger than that with horizontal, indicating that the B-X tunneling may become comparable with B-X-O MC for the viewing angles close to perpendicular.

[a]Model DP241-AB manufactured by Flann Microwave.

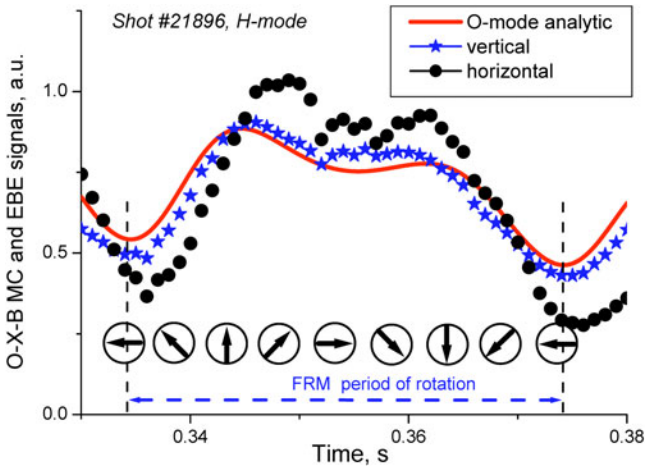

Fig. 2. B-X-O mode coupling efficiency at 16 GHz during one period of FRM rotation calculated analytically and 16-GHz EBE signals measured at vertical and horizontal polarizations simultaneously. EBE signals were normalized to radiative temperature estimated from TS measurements at the EBE origin.

These observations prove that the predominant fraction of these signals can be attributed to the mode-converted EBE. Indeed, the amplitudes of the radiometer signals correspond to radiative temperatures of several hundred electron-volts, indicating that emission comes from the plasma core. Typical ELM-free H-mode plasma in MAST has a very flat electron density profile, with central temperature ~1 keV and central density $\sim 5 \times 10^{19}$ m^{-3} ($\omega_{pe} = 63.5$ GHz). Hence, at typical toroidal magnetic field of 0.6 T ($\omega_{ce} = 16.8$ GHz), EC harmonics up to the third are blocked by cutoffs, prohibiting central EC emission completely. At the same time the observed signals are dramatically suppressed during ELMs, which disturb only the pedestal region of the plasma where MC occurs. All these observations support the EBE nature of the signals measured. However, the magnitude of the contribution from stray radiation is not clear.

To estimate the stray radiation fraction, we assume that stray emission is isotropic and is proportional to EBE and that its fraction is independent of frequency. The maximum peak signal and modulation depth due to FRM rotation is expected if the viewing trajectory was crossing the maximum of MC. Modulation, up to a factor of 4, is usually observed for frequencies from 13 to 15 GHz (see Fig. 3). At these frequencies dual maxima disappear, which means the optimum direction is just outside the scanning range that makes modulation stronger. This requires the stray radiation fraction to be not higher than 10%; otherwise, the shape of the signals cannot be reproduced by WKB MC simulation or full-wave modeling. Two important conclusions can be drawn from experimental signals presented in Figs. 2 and 3. The radiometer signals indeed correspond to the B-X-O mode-converted EBE. The B-X-O MC window is wider than estimated using density gradients from TS measurements directly. The edge gradient is usually smoothed due to the finite size of the scattering volumes. To account for the difference, the edge TS profiles have been fitted using a modified hyperbolic tangent (mtanh) function convoluted with the instrument function representing the spatial resolution of the diagnostic. The modified TS profiles agree well with EBE measurements.

Figure 3 represents EBE signals obtained on MAST during ELM-free period of H-mode in a range of frequencies covering EBE originated from the fundamental EC resonance, as illustrated in Fig. 4a. The X's indicate viewing orientations when the viewing angle tilt was close to the pitch angle. The radial position of the corresponding MC layer is found from high-resolution TS measurements (see Fig. 4a). As a first approximation WKB modeling of the MC process[13] was used for reconstruction of the pitch angle profile from EBE data. The WKB model reproduces well the shape and general behavior of the EBE signals, indicating that the O-mode contribution is predominant. The magnetic pitch angles were reconstructed using the best-fit method between the data and the simulated signal.

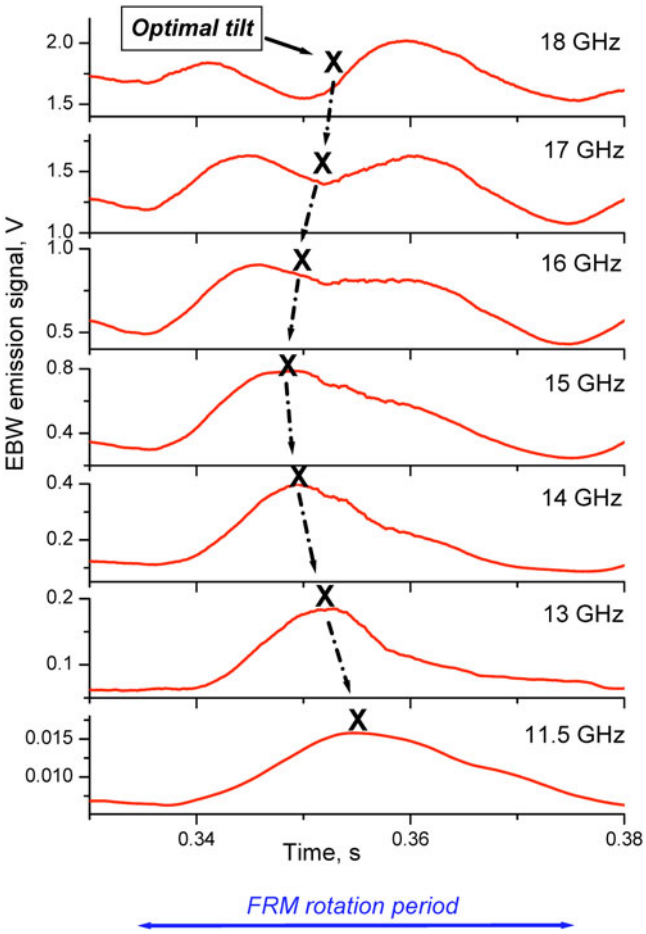

Fig. 3. EBE signals measured during one FRM rotation period, shot #21896. EBE in the frequency range 11.5 to 18 GHz predominantly originates from ω_{ce} resonance. The tilt of FRM corresponding to the MC plane is indicated by an X for each frequency.

The pitch angle reconstruction from EBW measurements in comparison with the motional Stark effect (MSE) diagnostic is shown in Fig. 4b. One can see that all the EBE data lie in a very narrow ~1-cm layer and indicate dramatic changes in the magnetic pitch angle within this layer. The estimated total field variations in the pedestal region can be seen in Fig. 4a from the behavior of EC resonance curves. Similar but less accurate results were obtained earlier from EBE spectroscopic measurements on MAST (Ref. 9). The WKB results have been verified with the full-wave analysis. This analysis was based on the reciprocity theorem[14] and included Gaussian beam propagation from the antenna to FRM, reflection from FRM, propagation through the vacuum window to the plasma boundary, and a solution of the full-wave one-dimensional MC problem with further multiray EBW ray-tracing until complete absorption within the plasma.[4,15] Finally, the signal received by the antenna was calculated as the sum of the signals estimated for the individual EBW rays.

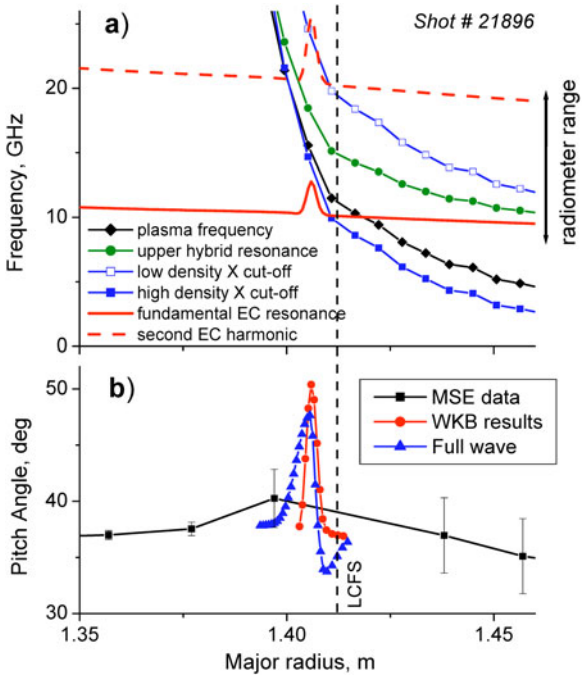

Fig. 4. Shot #21896: (a) Midplane topology of resonances and cutoffs near the plasma boundary. (b) Magnetic pitch angle measured with MSE and reconstructed from EBE in the framework of WKB approximation and full-wave analysis. Relative accuracy of the full-wave reconstruction is ~1 deg.

This procedure was repeated for a number of FRM angles over the rotation period and the simulated signal obtained in this way was compared with that measured by the radiometer. The magnetic pitch angle profile was reconstructed using the best-fit technique between simulated signals and experimental data at all available frequencies simultaneously. In general, the WKB reconstruction and the full-wave analysis are in good agreement. The full-wave analysis suggests that the pitch angle increase starts at smaller major radii and that the whole pitch angle perturbation is wider than inferred from the WKB reconstruction. Measurements at higher frequencies (up to 40 GHz, EBE from $3\omega_{ce}$), corresponding to MC layers located deeper in the plasma, show good agreement with MSE data. EBE results come into agreement with MSE measurements outside the last closed flux surface (LCFS) as well. However, EBE measurements show details of pitch angle variation within a narrow region just inside the LCFS (see Fig. 4b). These details occur on a scale length much shorter than the MSE spatial resolution; hence, they cannot be resolved by this diagnostic. EBE measurements averaged over the radial interval from 1.39 to 1.41 m, which corresponds to the MSE collection interval for this discharge (spatial resolution), give the same figure as measured by the MSE method.

To reproduce such behavior of the magnetic pitch angle, one would require a double-layer current sheath with each layer ~1-cm thick and with the currents flowing in opposite directions. The inner layer would carry the current in the same direction as the plasma current and the outer layer in the counterdirection. The current density required to match the amplitude and the shape of the pitch angle peak is ~3.2 MA/m^2 in the inner layer and about −2.8 MA/m^2 in the outer layer. The neoclassical current density estimated from TS measurements is typically ~1 MA/m^2 flowing in the codirection. Unfortunately, at the present moment we cannot provide a self-consistent explanation of these results. However, the pitch angle peak was observed in every ELM-free H-mode plasma shot, allowing reliable pitch angle recovery from EBE measurements, and the magnitude of this effect is certainly higher than the errors of measurements and reconstruction.

Temporal resolution of this technique based on mechanical scanning of the radiometer viewing angle is limited by the maximum speed of FRM rotation. At present it is ~10 ms. Relative accuracy of the pitch angle reconstruction is about 1 deg for the ELM-free H-mode plasma. Pitch angle reconstruction becomes very difficult or even impossible in the presence of magnetohydrodynamic (MHD) activity. This is the main limitation of this technique.

III. EBE IMAGING DEVELOPMENTS

Angular scanning EBE measurements have demonstrated the possibility of magnetic pitch angle reconstruction from the EBE angular distribution. Microwave imaging of the B-X-O MC window is proposed as an alternative to the mechanical angular scanning with FRM. The proposed scheme is based on the phased array technique, allowing the required angular resolution to be achieved in MAST experiments. Image acquisition time can be much shorter than MHD time scales, so the EBE imaging technique can potentially be used for pitch angle measurements in the presence of plasma instabilities, for example, to measure pitch angle evolution due to ELMs.

To exploit this possibility on MAST a microwave imaging system (MIS) is being developed in collaboration with York University. MIS consists of an array of antennas and relies on two methods of microwave image acquisition widely used in radio astronomy, namely, aperture synthesis and phased array techniques.[16] A triple-antenna prototype has been assembled to conduct initial tests with a microwave noise source (see Fig. 5) in the lab. Each antenna receives two polarizations in the frequency range from 6 to 40 GHz. Microwave signals are downconverted using heterodyne techniques and the intermediate frequency (IF) signals are digitized in a full-vector form at a sampling rate up to 500 megasamples per second. The

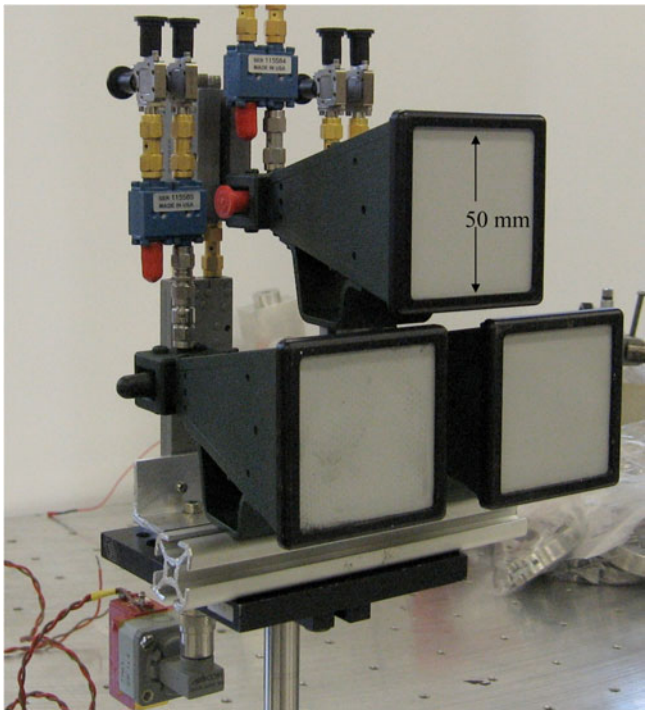

Fig. 5. Triple-antenna assembly prepared for EBE imaging lab tests with the noise source.

triple-antenna prototype was tested with the noise source and then calibrated with a monochromatic source against phase and amplitude balance across all channels.

Finally, the triple-antenna system has been installed on MAST and pilot plasma experiments have been conducted at a fixed frequency of 17.4 GHz. The system showed extremely high resilience to electromagnetic pickup despite the proximity of the microwave components to the vacuum vessel (see Fig. 6). Experimentally achieved broadband signal-to-noise ratios were ~8 for L-mode plasmas. This figure was typically a factor of 2 higher for plasmas in H-mode. Preliminary analysis showed a high degree of coherence of signals received by different antennas. Typical cross-correlation coefficients between channels are in the range of a few percent. Further analysis of the data is in progress.

Several methods for inverting the antenna signals into an image have been identified. Broadly, they are

1. singular value decomposition (SVD) of the linear system[17]
2. Gaussian linear inversion from Bayesian statistics[18]
3. cross correlation of antenna pairs as a function of phase difference.

Several codes have been developed allowing the modeling of arbitrary antenna configurations, subject to both near-field and far-field sources. These codes have been used to compare the inversion methods mentioned above in the far field for low antenna number arrays, in the presence of noise, incoherence, and a variety of image shapes. The SVD and the mean of the Gaussian linear inversion produce indistinguishable results as far as we

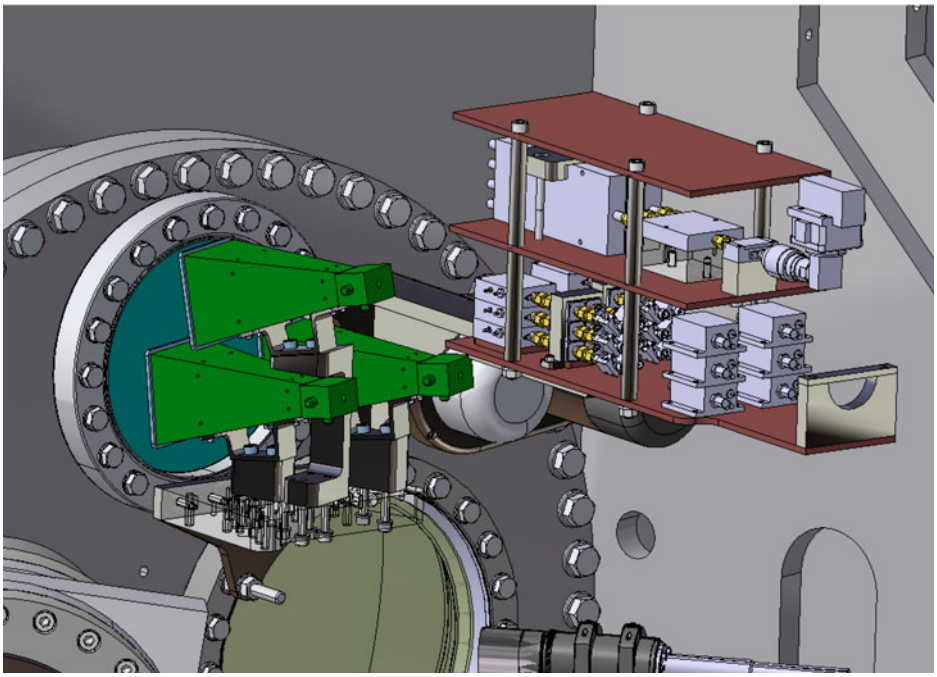

Fig. 6. Pilot experiment setup with the triple-antenna imaging system on MAST.

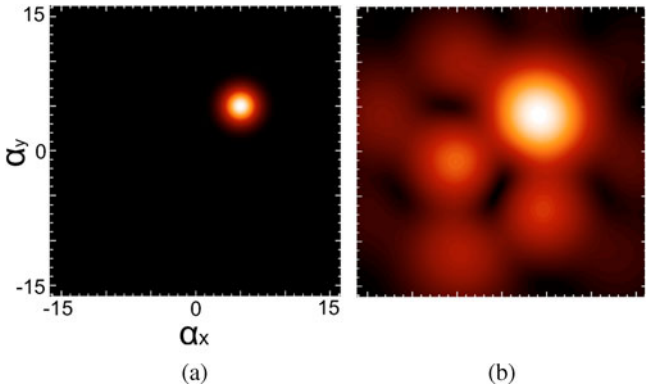

Fig. 7. (a) The microwave source used in modeling in angular coordinates (degrees) and (b) the response of a four-antenna Y-shaped array as reconstructed by SVD (right). Similar results can be obtained by the cross-correlation method, taking into account the antenna gain diagram.

can tell. The cross-correlation method has no inbuilt sidelobe suppression like the SVD, but it is far more resilient to noise. For many antenna arrangements it was found that the array was able to resolve the position of the center of the source very well, better than a factor of 10 over the diffraction limit of the array, as illustrated in Fig. 7. However, for some array configurations information about the width of the source could not be recovered using these techniques.

For the SVD, the image is a linear combination of what are known as "dual beams" formed from the eigenfields of the system,[17] and these dual beams are a property of the array only (see Fig. 8). Analysis of these beams allows us to predict the information to which the array will be sensitive. This provides an effective way to design the array configuration. This method of design makes it clear that in order to have sensitivity to the source width, antenna pairs must have unequal spacing. With three antennas, only the position of the source maximum can be reconstructed.

Additional information about the source shape can be gained by performing a deconvolution on measurements of power from each antenna. Since each antenna may be pointed at a slightly different angle and the emission may be modeled by a bivariate Gaussian, using the position measurements from the phased array allows resolution of the necessary two covariances and rotation angle to define this bivariate image Gaussian using only four antennas.

The final MIS system will have 36 Vivaldi-type antennas, 18 for vertical and 18 for horizontal polarization. The Vivaldi antennas are expected to be operational in the frequency range from 10 to 40 GHz. Only 8 of 36 antennas will be connected simultaneously to 8 available detector channels. Different combinations of operational antennas can be exploited on a shot-by-shot basis. First experiments with MIS using a multiple antenna array are planned on MAST in 2011.

IV. CONCLUSIONS

For the first time we have demonstrated experimentally that the magnetic pitch angle profile at the plasma edge in STs can be measured using thermal EBE. EBE escapes from the plasma via linear MC into electromagnetic modes. MC is efficient only in particular directions totally defined by the density gradient and magnetic field within the MC layer. This makes thermal EBE highly anisotropic. Two-dimensional measurements of EBE at several frequencies together with high-resolution density profile measurements allow the reconstruction of the magnetic pitch angle profile.

Mechanical angular scanning of thermal EBE has been conducted in MAST as a proof-of-principle of the

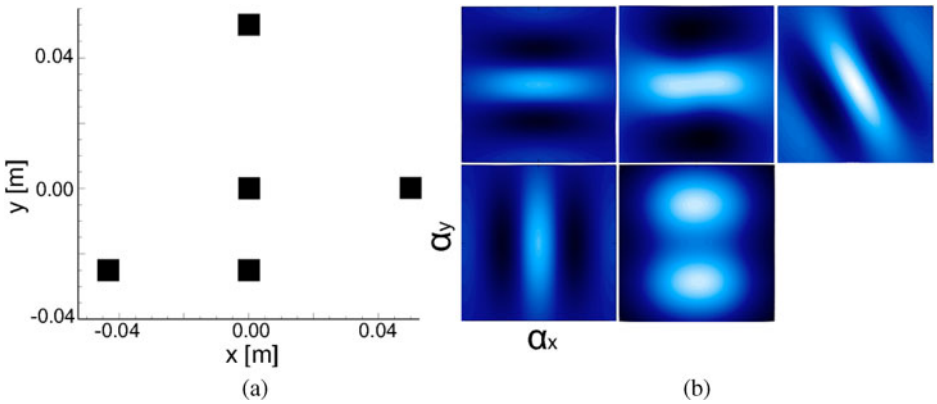

Fig. 8. (a) Five-antenna array with unequal spacing and (b) contour plots of the "dual beams" simulated for this array as described in Ref. 17. Angular range is ±30 deg in both directions. Dual beams show that such an antenna array provides information on the source width and it is most sensitive in the vertical direction.

method. The magnetic pitch angle profile has been reconstructed from EBE data and high-resolution TS measurements using full-wave MC modeling and EBW ray tracing. Results showed good agreement with MSE measurements. A subcentimeter spatial resolution and pitch angle accuracy of 1 deg has been achieved with the EBE measurements. In ELM-free H-mode plasma, pitch angle profiles reconstructed from EBE showed details not resolved by the MSE method. The EBE results reveal a bidirectional, radial current structure near the LCFS. The use of 2-D mechanical EBE scanning in present-day STs is very limited due to its poor temporal resolution. However, EBE scanning experiments provided a proof-of-principle for magnetic pitch angle measurements using 2-D EBE imaging. A fast 2-D microwave imaging system utilizing a phased antenna array is under development on MAST. This system will allow us to overcome time resolution limitations and will provide new insight into MC and plasma physics.

ACKNOWLEDGMENTS

This work was funded partly by the United Kingdom Engineering and Physical Sciences Research Council under grants EP/G003955 and EP/H016732 and the European Communities under the contract of Association between EURATOM and CCFE. The views and opinions expressed herein do not necessarily reflect those of the European Commission.

REFERENCES

1. A. DARKE et al., "MAST: A Mega Amp Spherical Tokamak," *Proc. 18th Symp. Fusion Technology*, Karlsruhe, Germany, August 22–26, 1994, Vol. 1, pp. 799–802, K. HERSCHBACH et al., Eds. (1994).

2. G. TAYLOR et al., *Phys. Plasmas*, **12**, 052511 (2005).

3. V. SHEVCHENKO et al., *Nucl. Fusion*, **50**, 022004 (2010).

4. V. SHEVCHENKO et al., *Fusion Sci. Technol.*, **52**, *2*, 202 (2007).

5. H. LAQUA, *Plasma Phys. Control. Fusion*, **49**, R1 (2007).

6. V. SHEVCHENKO, *Plasma Phys. Rep.*, **26**, *12*, 1000 (2000).

7. J. PREINHAELTER et al., *Rev. Sci. Instrum.*, **74**, *3*, 1437 (2003).

8. B. JONES et al., *Phys. Plasmas*, **11**, *3*, 1028 (2004).

9. J. URBAN et al., *Proc. 32nd Conf. Controlled Fusion and Plasma Physics*, Tarragona, Spain, Vol. 29C, P-1.121, EPS (2005).

10. F. VOLPE, *Rev. Sci. Instrum.*, **81**, 10D905 (2010).

11. V. SHEVCHENKO et al., *Proc. 17th Topl. Conf. RF Power in Plasmas*, Clearwater, Florida, AIP Vol. 978, p. 323 (2007).

12. F. VOLPE et al., *Proc. 15th Joint Workshop on ECE and ECRH*, Yosemite, California, p. 184 (2009).

13. R. A. CAIRNS and C. N. LASHMORE-DAVIES, *Phys. Plasmas*, **7**, *10*, 4126 (2000).

14. A. D. PILIYA and A. POPOV, *Plasma Phys. Control. Fusion*, **44**, 467 (2002).

15. A. N. SAVELIEV, *Plasma Phys. Control. Fusion*, **51**, 075004 (2009).

16. A. R. THOMPSON, J. M. MORAN, and G. W. SWENSON, Jr., *Interferometry and Synthesis in Radio Astronomy*, 2nd ed., Wiley (2004).

17. G. SAKLATVALA et al., *J. Opt. Soc. Am.*, **25**, 4 (2008).

18. O. FORD et al., *Rev. Sci. Instrum.*, **79**, 10 (2008).